The influence of grit blasting and UV/Ozone treatments on Ti-Ti adhesive bonds and their durability after sol-gel and primer application

Ardila-Rodríguez, Laura A.; Boshuizen, Bart; Rans, Calvin; Poulis, Johannes A.

DOI
10.1016/j.ijadhadh.2020.102750

Publication date
2021

Document Version
Final published version

Published in
International Journal of Adhesion and Adhesives

Citation (APA)
Ardila-Rodríguez, L. A., Boshuizen, B., Rans, C., & Poulis, J. A. (2021). The influence of grit blasting and UV/Ozone treatments on Ti-Ti adhesive bonds and their durability after sol-gel and primer application. *International Journal of Adhesion and Adhesives*, *104*, Article 102750. https://doi.org/10.1016/j.ijadhadh.2020.102750

International Journal of Adhesion & Adhesives 104 (2021) 102750

Contents lists available at ScienceDirect

International Journal of Adhesion and Adhesives

journal homepage: http://www.elsevier.com/locate/ijadhadh

The influence of grit blasting and UV/Ozone treatments on Ti-Ti adhesive bonds and their durability after sol-gel and primer application

Laura A. Ardila-Rodríguez [a,*], Bart Boshuizen [b], Calvin Rans [a], Johannes A. Poulis [a]

[a] Structural Integrity and Composites, Faculty of Aerospace Engineering, Delft University of Technology, Delft, 2629HS, the Netherlands
[b] Faculty of Applied Sciences, Delft University of Technology, Delft, 2629HZ, the Netherlands

ARTICLE INFO

Keywords:
Surface treatment
Titanium and alloys
Primers and coupling agents
Durability
Grit-blasting
UV/Ozone

ABSTRACT

In this study, different surface pretreatments were applied to clean and activate titanium alloy surfaces. The samples were subjected to grit blasting treatments using two different pressures and afterwards, a UV/Ozone treatment was applied at different times to study the wettability and surface oxidation of the titanium samples. Scanning electron microscopy and laser confocal microscopy showed the surface morphology and the increased roughness with grit blasting pressure. X-ray Photoelectron Spectroscopy revealed that titanium was increasingly oxidized with increasing UV/Ozone treatment time, which leads to a reduced contact angle and a better adhesive performance in a butt tension test proving the effectivity of this surface treatment for titanium. Furthermore, the addition of sol-gel AC-120 and corrosion inhibition primer BR 6747 showed to be an additional improvement in the initial adhesion and after different degrees of aging by exposure to salt-spray, making the surface treatment techniques used in this research, a promising environmental friendly alternative to improve adhesive bonding performance.

1. Introduction

Reducing weight with no sacrifice of mechanical performance to reduce the environmental impact and save operational and fuel costs has been an important research objective in the transportation industry. For many applications, the use of adhesive bonding is preferable because it avoids the increased weight of the mechanical fastening, such as riveting and bolting, and prevents the thermal affectation of the metal adherends as could happen as a result of welding [1]. The surface pretreatment carried out on an adherend before the application of the adhesive takes place is a determining factor in the success of the bonding process as a whole. Besides this, the pretreatment of metallic adherends should not only increase the adhesive bond strength but should also protect the metallic substrate from corrosion and thus improve the durability of the adhesively bonded joint, which is of great importance. Unfortunately, many of the most successful pretreatment process are also the most environmentally unfriendly due to the use of highly toxic chemical agents. This has led to efforts to search for new pretreatment methods that are more environmentally and economically friendly [2,3].

Surface pretreatment can typically be subdivided into various steps that can be combined to form the overall pretreatment procedure. One important step involves the texturizing of the adherend surface, typically through mechanical abrasion, which has three main benefits. First, it removes the loosely bound oxides from the adherend surface, second, it creates a fresh surface and third it increases the roughness (in microscale) of the surface to be bonded, thus increasing its contact area for bonding [4,5], and potentially creating the opportunity for some degree of mechanical interlocking between bonded adherends by the adhesive penetration into the created micro irregularities of the adhered's surfaces [6,7]. Two surface texturizing techniques that are found to be applied often in literature are grit blasting and abrasion [5,8,9]. Treating the surface changing blasting parameters such as blasting pressures and abrasive particle sizes leads to a different surface roughness which can influence the adhesive bonding performance. Laser surface texturizing has been used to change the metal surface and promote mechanical interlocking. Depending on the interaction between the laser process parameters and the material properties different textures can be generated modifying the surface topography. Kurtovic et al. [10] found that the laser pretreatment process performed in titanium alloy improved long term durability of adhesive bonds by the creation of a nanostructured oxide layer that leads to mechanical interlocking of the adhesive in the porous oxide layer.

* Corresponding author.
E-mail address: l.a.ardilarodriguez@tudelft.nl (L.A. Ardila-Rodríguez).

https://doi.org/10.1016/j.ijadhadh.2020.102750
Received 1 July 2020; Accepted 3 October 2020
Available online 9 October 2020

Surface pretreatment by chemicals is another common step in the surface pretreatment process. Anodizing processes, for instance, creates a fresh oxide layer on the metal surface as a result of the chemical dissolution of the metal and electrochemical oxidation of the surface. That anodic oxide layer has a high degree of micro-roughness which is desirable because of the tendency to form a mechanical micro composite interphase [11]. There are various electrolytes employed for the anodization process, including acid-based [8,12,13], fluoride-based [14], and hydroxide-based [2,15] anodization. However, the use of strong chemicals requires significant amounts of water to rinse the treated parts and additional hazardous waste that requires special handling and disposal. A process that can produce stable adhesive bonds with excellent results without the use of hazardous materials is the sol-gel method [16]. The *Si*–Zr based sol-gel is expected to form a film at the interface that bonds covalently between the metal titanium surface and the water-based primer as such improve the durability of the adhesive bond [17]. The last one is important, especially for metallic adherends, when environmental conditions might affect the lifetime of adhesively bonded joints by the diffusion of moisture to the adhesive-adherend interface, thus causing adhesive failure. An adhesive primer is typically used to protect the bonded adherend from moisture attack and improve long-term durability [9,18,19].

Regardless of the pretreatment, a clean, dry, and adhesion limiting contaminant's surface is always required for the adhesive bonding process. UV/Ozone treatment has been found to be a very effective cleaning technique in removing organic contamination. It is relatively simple, inexpensive, and strongly reduces chemicals consumption. In the UV/Ozone treatment, UV rays are absorbed by oxygen to form ozone and atomic oxygen and are simultaneously absorbed by most hydrocarbon substances. The organic chemistry contaminants suffer chain scissions by the incidental UV-light and are also decomposed by the formed ozone gas and highly reactive atomic oxygen species that act as a strong oxidizer [20]. The UV/Ozone treatment has been investigated for metals surface oxidation in semiconductor devices [21,22], and thin-film solar cells [23], as well as to oxidatively modify polymer surfaces for adhesive bonding applications [24]. However, it has been less studied as a method for improving the adhesion of a metal substrate to a polymer layer [25]. On this basis, the purpose of this research is to characterize the effect of grit blasting pressure and different exposure times to UV/Ozone treatment on the morphology, oxidation, and wettability of Ti6Al4V alloy to find the surface pretreatment that provides the lowest contact angle (thus the best wetting) and the best initial adhesive performance in a butt joint tension test. The durability of the adhesive bonding after sol-gel and primer application is also evaluated after 3, 6, and 12 weeks of corrosion aging in a salt spray chamber.

2. Methods

This study was carried out in two stages using butt tension specimens conforming to the ASTM D2094-00 (2014) [26]. In the first stage, various surface pretreatments comprising of a combination of grit blasting and UV/Ozone treatments were investigated, with grit blasting pressure and UV/Ozone exposure time being varied. The effectiveness of the pretreatments was quantified in two ways. First, the degree of surface activation was measured through contact angle measurements. Second, samples with different surface pretreatments showing lower contact angles were adhesively bonded and tension test performed. From these results, one parameter set was selected for further investigation within the second stage of the research. In this second stage, the durability of the bonded joints, applying sol-gel and primer, was investigated by tension test of the bonded specimens subjected to varying degrees of aging by exposure to salt-spray. This test method is supplemented with surface morphology and roughness measurements, X-Ray Photoelectron Spectroscopy and fractography to aid in the discussion and evaluation of the obtained results.

2.1. Materials

For the adherend material, 10 mm diameter Ti6Al4V Grade 5 rods supplied by Salomon's Metalen B·V (The Netherlands) were used. As a surface pretreatment sol-gel AC-130-2 supplied by 3 M and BR 6747-1 water-based corrosion inhibiting primer supplied by Solvay (USA) were used. Finally, the adhesive film was FM 94 K supplied by Solvay (USA) with a nominal weight of 293 gsm, a nominal thickness of 0.25 mm and polyester knit carrier.

2.2. Surface preparation methods

The titanium specimens were ground and cleaned with acetone. After that, the samples were subjected to various added surface pretreatments, such as sandpaper or grit blasting followed by various UV/Ozone treatment times. In the second half of the study, sol-gel and primer were applied to protect the surface of the samples to be tensile tested both in the initial condition (without aging) and aged.

2.2.1. Grinding

The titanium rods were cleaned with acetone before and after being ground with #320 followed by #600 SiC paper (Struers, Denmark) to remove the surface oxides and the patterning caused by machining. To grind the rods, the samples were mounted in a fabricated device (see Fig. S1a) to ensure the uniform abrasion and obtain plane and parallel surfaces, the pressure applied to the device during the grinding process was 5 N.

2.2.2. Grit-blasting

The titanium rods were cleaned with acetone before and after being grit blasted. The grit blasting pretreatment was carried out in a Pulsar 3 Clemco blasting cabinet (Clemco Industries Corp., USA). The abrasive material was white corundum iron-free quality Corublast Super Z-EW FEPA nr.100 (Leering Hengelo, The Netherlands) that was not recirculated during the process. The blasting pressure was set to 3 and 5 bar. The distance between the specimen and the gun was around 15 cm and the angle was set to 50° over the horizontal axis of the cabinet. After the grit blasting the samples were cleaned again with acetone to remove the bulk of organic contaminants and particles.

2.2.3. UV/ozone treatment

The UV/Ozone treatment was applied with three low pressure, ozone-generating UV- light tubes with a power of 30 Watt (UV Technik, Germany) at a distance of 10 mm from the specimen's surface for 5, 10, 20, and 40 min to find the optimal treatment time.

2.2.4. Sol-gel and primer application

Two surface preparations were applied to the adherends for the mechanical tests, once the best parameters of grit blasting pressure and UV/Ozone treatment time were determined. To improve the stability of the obtained surface and to achieve an optimal bond between the oxide layer and the adhesive, the AC-130-2 Sol-gel was applied. This was achieved by submerging the pre-bonded surfaces for 2 min in the sol-gel and allowing the part to drain for 10 min, there was no surplus to be removed. The surfaces were then dried for 30 min at room temperature and further cured at 60 °C for an additional 30 min. Finally, to achieve the optimum strength and durability, the BR 6747 primer was applied directly on top of the sol-gel as recommended by the supplier, using an air-atomizing gun. The samples were (again) dried for 30 min, after which they were cured at 121 °C for 60 min. The primer thickness measured by an Extech CG304 Coating Thickness Tester in Eddy-current working principle was 7.5 ± 2.71 μm.

2.3. Specimen preparation methods

From the original titanium rod, different specimen configurations

were made, depending on the type of test to be performed. Short titanium rods were used for surface characterizations, standard titanium adherends were built to manufacture the adhesive-bonded specimens.

2.3.1. Specimen details

For the easy handling of the samples inside the equipment during the study of the surface morphology, roughness, chemistry, and wettability, Ti rods were cut to 5 mm in length and the surface prepared as described in sections 2.2.1 and 2.2.2. For the adhesive bonding, the titanium adherends were built up according to the ASTM standard D2094-00 (2014) which final dimensions and shape are presented Fig. 1a.

2.3.2. Manufacturing process of adhesively bonded specimens

The adhesive bonding process was performed by laying the uncured film adhesive, cut with a stamp tube in rounded parts of 10 mm diameter, between two titanium adherends previously prepared with the methods as described in section 2.2. After that, the adherends were aligned at 90° (Fig. 1a), with the help of the pre-fabricated fixture shown in Fig. 1b, as suggested by ASTM D2094-00 (2014). A vacuum setup was arranged around the alignment device and the curing process was performed as recommended by the supplier in a Scholz autoclave (Scholz Autoclaves Maschinenbau Scholz GmbH & Co. KG, Coesfeld, Germany) at 2.8 bar pressure and 121 °C curing temperature during 60 min with heating and cooling rates of 1 °C/min. The bonding process of the adherends was performed within 30 min after the surface preparation.

2.4. Test and measurement methods

The treated surfaces were studied in terms of obtained morphology and roughness, chemical state and wettability, and the adhesively bonded samples were tensile tested, and the failure mode identified.

2.4.1. Surface roughness and morphology

The surface morphology of the treated specimens was analyzed using a JEOL7500F (JEOL, Japan) Field Emission Scanning Electron Microscopy (FESEM) in Low Magnification mode and Lower Secondary Electrons detector (LEI) with 5.0 kV, working distance of 15 mm and a vacuum of 9.6×10^{-5} Pa. A Keyence Laser scanning Confocal Microscope (Keyence International, Mechelen, Belgium) was used to evaluate the surface roughness of the treated samples by the S_a parameter (arithmetical mean height). The surface texture parameter S_a expresses an absolute value, the difference in height of each point compared to the arithmetical mean of the surface in the definition area.

2.4.2. Surface chemistry

Information on the chemical composition of the surfaces of the treated specimens were obtained by X-ray Photoelectron Spectroscopy (XPS), using a K-alpha Thermo Fisher Scientific (USA) spectrometer and a monochromatic AlKα X-ray source with an X-ray spot size of 400 μm. Survey spectra were initially acquired followed by the acquisition of high-resolution Carbon (C 1s), Oxygen (O 1s), Aluminum (Al 2p) and Titanium (Ti 2p) spectra. The measurements were performed at ambient temperature and chamber pressure in the order of magnitude of 10−7 mbar. A flood gun is always used for charge compensation. The electron energy analyzer was operated with a pass energy of 200 eV for survey spectra and 50 eV for high-resolution spectra. Each high-resolution spectrum was scanned 10 times. The spectra were analyzed and processed using CasaXPS software and the average value of two separate measurements was taken as the result with the reported standard deviation being not higher than ±1% At.

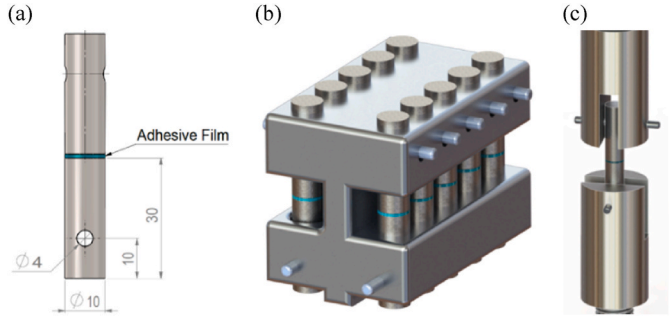

Fig. 1. (a) Titanium adherend with dimensions in mm, (b) Alignment Fixture, (c) Tensile test grips setup.

2.4.3. Contact angle

Contact angle measurement (CAM) was used to evaluate the wetting properties of the surface pretreatments listed in Table 1 following the procedure described in Section 10 of the ASTM D7490-13 [27]. The contact angle of a 5 μl distilled water drop was measured on both sides 6 times using a Technex Cam200/Attension Theta V4.1.9.8 system (TECHNEX BV, Wormerveer, The Netherlands) and was taken by curve fitting the droplet profile and measuring the angles formed between the tangents of the fitted curve and the horizontal axis. The average value of the separate measurements was taken as the result.

2.4.4. Tensile strength

The butt tension tests were performed on a Zwick-Roell test machine (Zwick Roell Group) with a 10 kN load cell, where five specimens per configuration were subject to a tensile loading test following the ASTM standard D2095-96 (2015) [28]. The test was conducted at room temperature and 55% RH at a speed of 0.5 mm/min and the maximum load carried by the specimen at failure was recorded, Fig. 1c is a schematic representation of the test setup grips. To correct the axial alignment during the test, a cardan was connected to the test machine (see Fig. S1b). The tensile strength was calculated by dividing the breaking load by the area of the bonded surface. Both the arithmetic mean obtained from the five repetitions per test and the standard deviation are reported.

2.4.5. Fractography

To assess the initial adhesion properties, the inspection of the fracture surface was conducted in a Keyence VR-5000 wide-area 3D measurement system (Keyence International, Mechelen, Belgium), using an enlargement of 25x. The remaining adhesive film area on both adherends after failure was measured using the Adobe Photoshop CC 2018 Color Range function, and the percentage of remaining adhesive calculated using Equation (1), where the values closer to 100% are indicative of cohesive failure and values closer to 0% indicate of more adhesive failure, values in-between indicating a mixed-mode failure. For the tensile strength and adhesive percentage, the mean value and standard deviation were used for statistical analysis.

$$\%\ of\ remaining\ adhesive = \left[\frac{remaining\ adhesive\ film\ area\ on\ both\ sides}{total\ bonding\ area}\right] \times 100$$

Equation 1

The sequence in which the methods, described in the previous sections, were used to select a grit blasting pressure and the UV/Ozone treatment time parameter (S) are summarized in Fig. 2.

2.4.6. Aging: salt spray exposure

The durability of the adhesive bond was evaluated by salt spray exposure following the recommendations of the ASTM B117-18 standard [29]. The adhesive bonded specimens, using the selected surface pretreatment parameter combined with sol-gel and primer, were exposed to a neutral 5 wt% NaCl fog at 35 °C in a Liebisch Constamatic Salt Spray chamber (Gebr. Liebisch GmbH & Co. KG, Bielefeld, Germany) during 3 weeks (500 h), 6 weeks (1000 h), and 12 weeks (2000

Table 1
Specimens description.

Parameters	Sample												
	P-0	P-1	P-2	P-3	P-4	P-5	P-6	P-7	P-8	P-9	P-10 S[1]	SSG[1]	SSGP[1]
Ground	X												
Grit Blasting Pressure (bar)		3	3	3	3	3	5	5	5	5	5	5	5
UV/Ozone Time (min.)		0	5	10	20	40	0	5	10	20	40	40	40
Sol-Gel AC-130-2												x	x
Primer BR 6747-1													x

S: Selected Parameter
[1]Samples exposed to Salt Spray.
SSG: Selected parameter combined with Sol-Gel
SSGP: Selected parameter combined with sol-gel and primer.
Samples grey-coloured were tested by butt joint tension test.

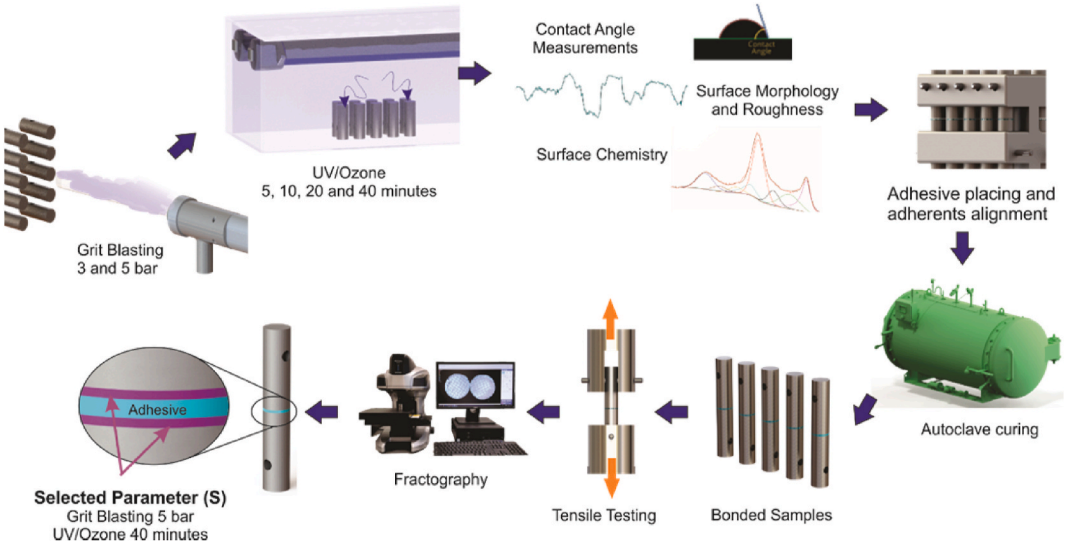

Fig. 2. Surface pretreatment sequence to parameter selection.

h). The tensile strenght and fracture surface analysis, as described in sections 2.4.4 and 2.4.5, were conducted to the samples before and after salt spray exposure at each time interval and the mean value and standard deviation were used for statistical analysis. Fig. 3 summarizes the procedures to access the adhesive bonding after salt spray exposure.

2.4.7. Test matrix

A summary of the surface preparation methods applied and the names given to the specimens are presented in Table 1. All samples were pre-cleaned with acetone prior to the surface pretreatments. Sample P-0 is the titanium rod just ground with SiC paper as described in the first part of section 2.2.1, this sample is used for reference purposes. Samples P-1 to P-10 are the samples prepared as described in sections 2.2.1 and 2.2.2. With different grit blasting pressures and UV/Ozone exposure times. Test and measurement methods described in section 2.4.1 to 2.4.3 were necessary to evaluate samples P-0 to P-10. From this group of results, samples P-3, P-5, P-8, and P-10 were selected to assess the adhesive bonding performance as described in section 2.4.4. Finally, sample P-10 showed the optimum parameters (S) to be applied in combination with sol-gel and primer in the samples exposed to salt spray (section 2.4.6).

Fig. 3. Adhesive bond quality assessment sequence after salt spray exposure.

3. Results and discussion

3.1. Surface morphology and roughness

After grit blasting the surface roughness of the titanium was measured. Fig. 4 presents the roughness profile and a view of some surface pretreatments together with the measured surface roughness parameter S_a. In Fig. 4a, the roughness profile curve is smoother and the color of the surface image is homogeneous compared to the grit-blasted samples (Fig. 4b and c). Comparing the roughness parameter S_a presented in Fig. 4, it is observed that the roughness of the sample ground **with** SiC sandpaper (P-0) is much less than the results for the grit-blasted 3 bar (P-1) roughness. This implies that the grit blasting has a significant effect on the surface roughness. Fig. 4b and c shows the influence of the grit-blasting pressure on the surface morphology. As the pressure increases from 3 (P-1) to 5 (P-6) bar, the abrasive material interacts more strongly with the substrate creating deeper and irregular grooves and ridges on the surface and as a result the value of the surface roughness increases in comparison to the surface roughness of sample P-1. This increased roughness as a result of the grit blasting pressure was also shown by Li et al. [5]. When sandblasting aluminium-lithium alloy. The surface roughness of the samples treated with different UV/Ozone treatment times does not present a noticeable change in the roughness parameters, as expected from these short exposure times, and this resolution.

Fig. 5 shows the SEM images of the surface morphology of the samples. The surface ground by SiC paper shown in Fig. 5a, appears to be flat with only some minor scratches, and from the results already presented in Fig. 4, it is shown that, indeed, this sample has the lowest surface roughness. On the contrary, the grit-blasted samples surface morphology is prominent with elevations and valleys. This morphology is developed due to the high-speed impact of the abrasive onto the surface of the samples during the grit-blasting, deforming the material, and creating depressions with different sizes and irregular shapes. Fig. 5b presents the sample grit blasted with 3 bar of pressure, it shows a sharp and random profile full of peaks and valleys homogeneously distributed, compared with Fig. 5c where the valleys appear to be deeper and stretched, with apparently higher deformation caused by the increased pressure.

3.2. Contact angle measurements

The static contact angle values summarized in Fig. 6 clearly show the modification of the titanium surface following surface pretreatments. As can be seen, the contact angle of the "ground by sandpaper only" sample (P-0) was around 98.2°. After the "as received" samples had been grit blasted and cleaned by acetone, the contact angles present a significant reduction of the contact angle values being 65° and 58.4° for 3 bar (P-1) and 5 bar (P-6), respectively. Such reduction can be explained by the removal of organics after cleaning with acetone. On the other hand, it is observed that the rougher the surface, the smaller the contact angle, when comparing the grit-blasted samples (P-1 and P-6) to the same surface in a smooth state (ground only sample or P-0). This change in the contact angle could partly be associated with the remaining abrasive material in the surface after grit-blasting (See Fig. S2) but, as was showed by Wenzel [30], is related to the roughness factor. Roughening the surface increases the surface free energy and consequently the extent of wetting. The morphology and increased roughness created by the grit blasting increase the contact area between the liquid and the surface leading to apparent higher surface energy and a smaller contact angle

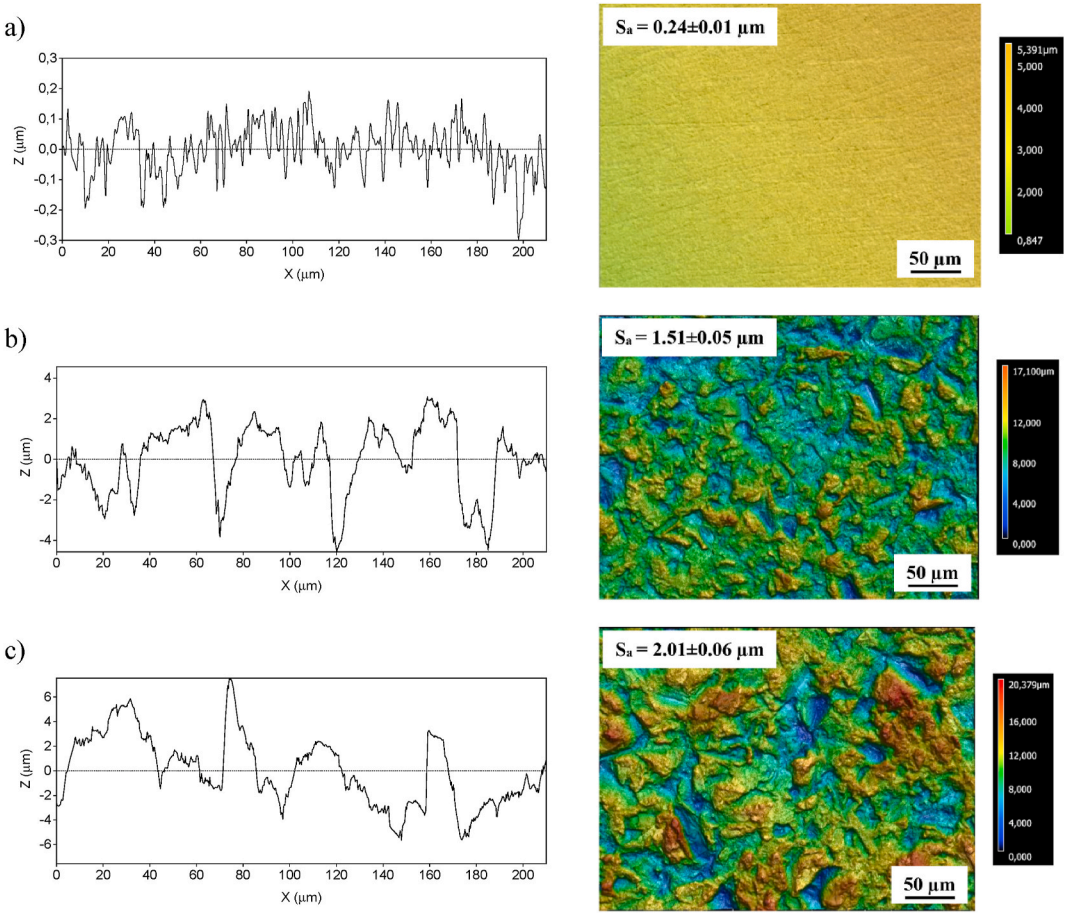

Fig. 4. Roughness profile and Surface Roughness of Ti6Al4V treated with (a) P-0, (b) P-1, (c) P-6.

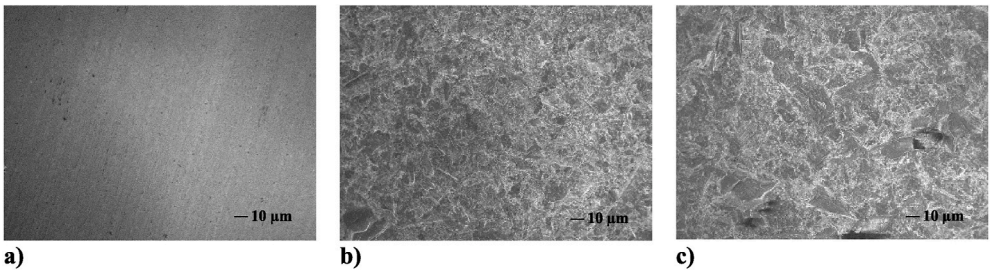

Fig. 5. SEM images showing the Titanium surface morphology: (a) P-0, (b) P-1 and (c) P-6.

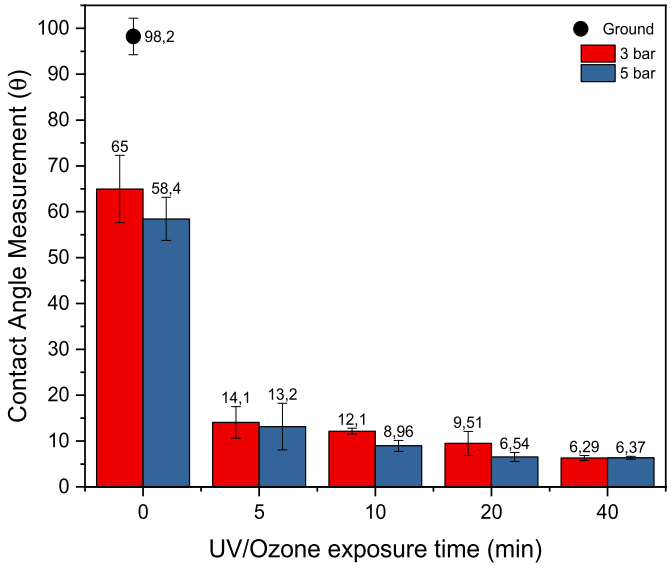

Fig. 6. Contact angle measurements with two different blasting pressures at various UV/Ozone exposure times.

[7]. The difference between the contact angles obtained for the samples grit blasted with 3 and 5 bar pressure is more pronounced at lower UV/Ozone exposure times with lower average angles for the 5 bar treated samples. However, this difference is not significant within the standard deviation.

In addition to acetone cleaning and grit blasting, the 5 min UV/Ozone treatment reduces the contact angle values to 14.1° (P-2) and 13.2° (P-7). As UV irradiation time increases, the contact angle values of samples grit blasted with 3 and 5 bar are reduced to ~6° by increasing the UV/ozone treatment time to 40 min [24]. This reduction is a consequence of the removal of the last traces of organic contaminations [20], followed by changes in the surface composition induced by the UV/Ozone treatment due to titanium oxidation [31], which have been studied by XPS.

3.3. Surface chemistry

XPS measurements were carried out to assess the evolution of the surface chemistry of the samples as a result of the different pre-treatments. The results are summarized in Fig. 7 a - d.

Fig. 7a shows the surface atomic percentages of oxygen, carbon, titanium, and aluminium obtained from the survey spectra for each sample. Vanadium is located beneath the top surface and may only be observed by XPS after some sputtering. The sample P-0 ground with SiC paper has an oxygen content of ~44%, attributed to the native oxide formation on the surface of the titanium. The grit blasted only sample (P-6), shows a slow reduction of the oxygen content. Although grit blasting is expected to remove the native oxide layer of the metal, the oxygen

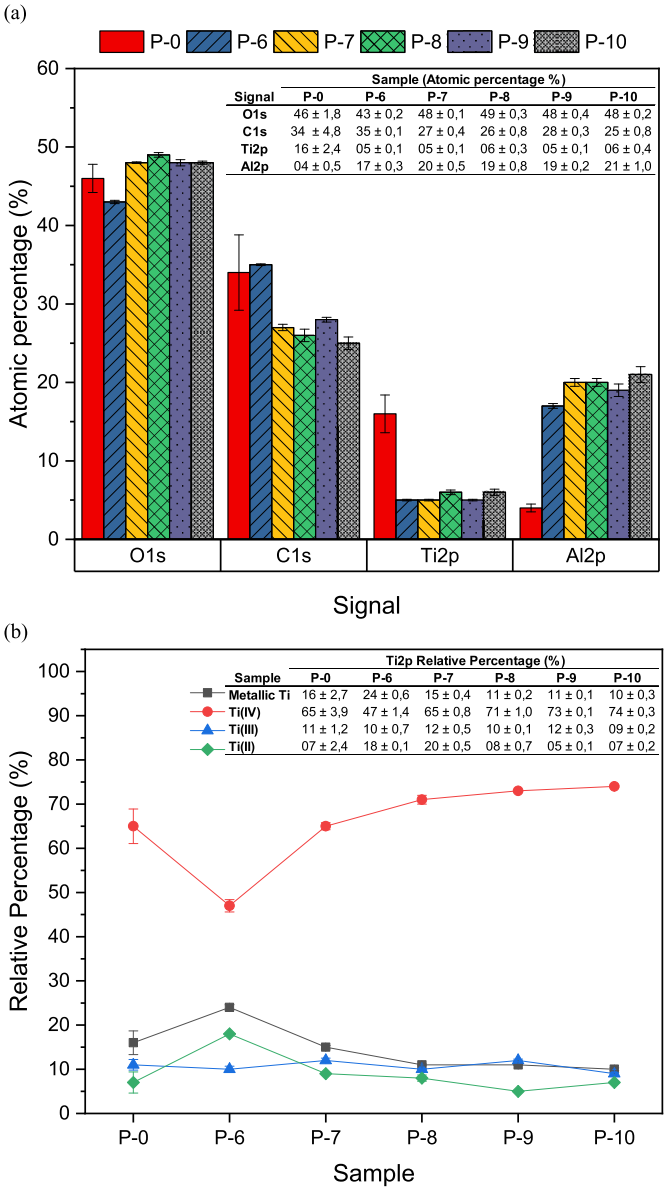

Fig. 7. (a) XPS surface atomic percentages, (b) Relative percentages obtained for Ti2p high-resolution spectra.

content is not reduced since some corundum residues associated with the grit blasting procedure have been deposited onto the surface [9]. This observation is supported by the Ti2p and Al2p percentages. The titanium percentage of the ground sample (P-0) is ~17% and for the grit-blasted samples (P-6 to P-10) this is reduced to less than 6%, while the aluminium percentage is increased to 20.6%, respectively. The

percentage of atomic oxygen in the surface of the UV/Ozone treated samples (P-7 to P-10) is increased to ~48% suggesting the surface oxidation of the samples. At the same time, the UV/Ozone treated samples show a decrease in the surface carbon content compared to the ground (P-0) and grit blasted (P-6) samples. This reduction is expected to be a result of the cleaning effect of the UV/Ozone [20]. Further information on the chemical modifications resulting from the UV/Ozone treatment can be obtained by analyzing the high-resolution spectra of Ti2p. A summary of the results from the peak fits is presented in Fig. 7b. The high-resolution spectra of Ti2p revealed the combination of four XPS doublet structures attributed to Ti(IV) (458.4 and 464.1 eV), Ti(III) (456.8 and 462.6 eV), Ti(II) (455.1 and 460.8 eV) and Ti (0) (453.3 and 459.4 eV) corresponding to TiO_2, Ti_2O_3 or Ti_3O_5, TiO, and metallic Ti, respectively [32,33]. After 40 min of UV/Ozone treatment, as observed in Fig. 7b, the contribution of metallic Ti, and Ti(II) decrease. Ti(III) shows slight variations but in general, remains constant, and Ti(IV) strongly increases to 74.7%. Ti(IV) arises at the surface of the Ti alloy at the expense of metal atoms and sub-oxide ions Ti(II), that react with the oxygen ions to form Ti(III) and Ti(IV) [32,34]. The increase in Ti(IV) with treatment time, also visualized comparing Fig. 7c and d, suggests the utility of the UV/Ozone treatment as a preparation step to improve the adhesive joints behaviour [31].

3.4. Adhesive bond performance

It is expected that the lower contact angle values show a better initial adhesive joint performance due to an increased wetting [5,6]. However, the relations between roughness, wetting and adhesion are complex and the adherend surface topography that improves the adhesion depends also on the adherend surface chemistry [4,35,36]. To assess this assumption, samples prepared with 3 and 5 bar of grit-blasted pressure and irradiated with 10 min (P-3 and P-8) and 40 min (P-5 and P-10) of UV/Ozone were adhesively bonded and mechanically tested. The tensile strength of the bonded joints and the failure surfaces were evaluated and the results are presented in Fig. 8.

The tensile strength results are summarized in Fig. 8a. It can be seen that there was not a significant difference between the bond strength of the tested samples regarding the surface roughness as a result of the grit blasting pressures nor as a result of UV/Ozone treatment time. The failure surfaces of the samples P-3, P-8, and P-5, were photographed after the tensile test and are presented as a typical example in Fig. 8c. In this figure, there is an interfacial failure, where the areas of the lacking adherend are the counterparts of the areas with adhesive. However, as seen in Fig. 8d for the sample P-10, grit blasted with 5 bar and irradiated with UV/Ozone during 40 min, there are areas where the layer of adhesive remains on both adherend surfaces, which indicates cohesive failure together with some other areas showing adhesive failure. Sample P-10 presents a mixed failure mode and shows to be the best-observed failure type for these tests. Fig. 8b summarizes the results of the calculations obtained by Equation (1). These percentages show more accurate information on the effect of the surface pretreatments applied. Comparing the obtained percentages for the samples when grit blasted with either 3 or 5 bar. It is seen that the trend to cohesive failure is higher for the samples grit blasted with 5 bar of pressure (samples P-8 and P-10). On the other hand, analyzing the effect of UV/Ozone irradiation time, it is observed that there is a notable difference for the sample P-10, grit blasted with 5 bar of pressure and exposed during 40 min of UV/Ozone. This sample, unlike the ones treated by the other three conditions, reached a percentage of about 66% (Fig. 8d); a more mixed type of failure. The morphology can increase the adhesive bond quality when complemented with the oxidized surface obtained from a longer UV/Ozone irradiation time, as indicated by XPS analyses in the previous section.

3.5. Salt spray aging test

Test samples (see Table 1) were exposed to salt spray fog during either 3 weeks (500 h), 6 weeks (1000 h) and 12 weeks (2000 h) to determine the durability of the adhesive joints. From the results obtained in the previous sections, 5 bar grit blasting in combination with 40 min of UV/Ozone pretreatment were found to be the optimum parameters (S) to prepare the samples for the aging evaluation. To improve the stability of the adherend's surface and to achieve the optimum strength and durability, Sol-gel AC-130-2 (SSG) and the BR 6747-1 primer (SSGP) were applied. The results obtained for three different surface preparations and evaluated after 0, 3, 6, and 12 weeks are compared in Fig. 9.

Fig. 9a presents the obtained results of the tensile strength. For the samples without aging (0 weeks), the tensile strength is higher than those of all the aged ones. Though the optimum parameter (S) treated

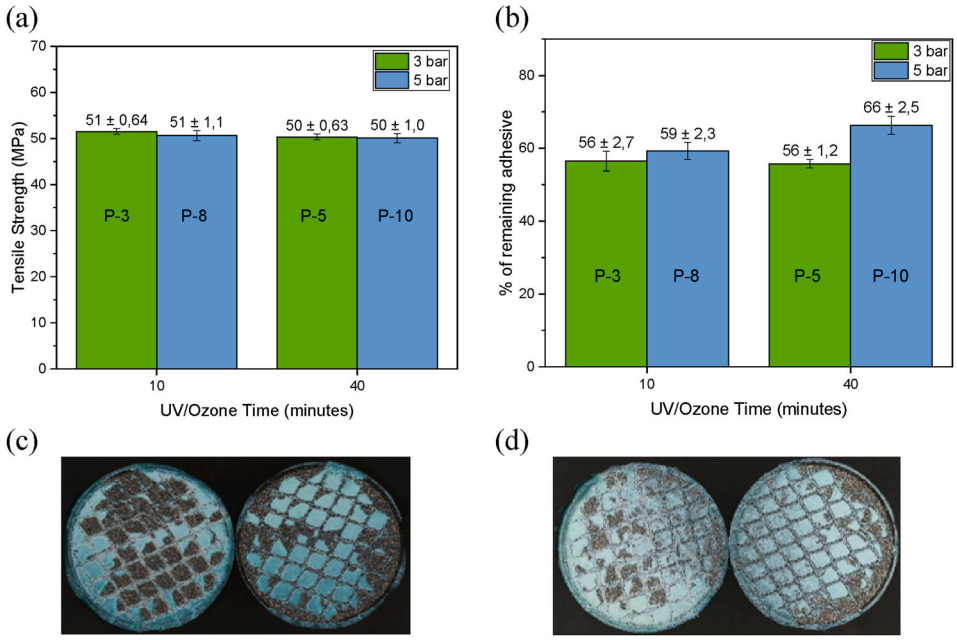

Fig. 8. (a) Tensile strength, (b) percentage of remaining adhesive, fractured surface of (c) P-5, and (d) P-10.

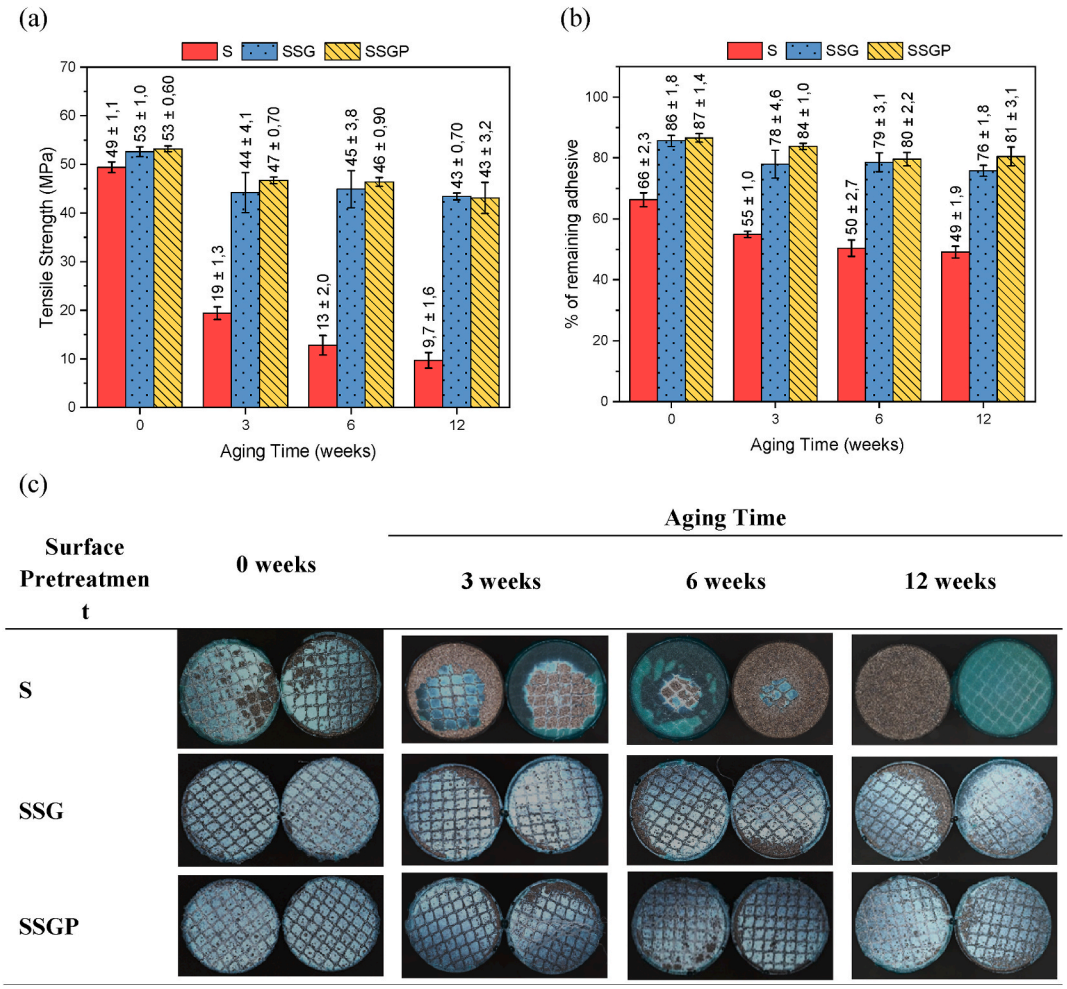

Fig. 9. (a) Tensile strength, (b) percentage of remaining adhesive, and (c) fractured surfaces after 0, 3, 6, and 12 weeks of salt spray exposure.

surfaces showed a lower tensile strength (49 MPa) than both the sol-gel (SSG) only as well as the sol-gel and primer treated samples (around 53 MPa). Meaning that the tensile strength increases by adding sol-gel and/or primer.

After 3 weeks of aging, there is a huge reduction in the average tensile strength for the sample with the selected parameter (S) only, that drops to almost 40% of its initial value after 3 weeks of salt spray testing. With 6 and 12 weeks of aging, the tensile strength was again further reduced, which is also in line with the increased adhesive failure type that occurred. The tensile strength values obtained for the samples with sol-gel and primer treatment show a much less severe reduction. After 12 weeks, the tensile strength was about 10 MPa for the selected parameter only, but still about 43 MPa for the sol-gel and primer combination, showing just a slight drop compared with the initial values of tensile strength in the aging times previously mentioned.

Surface preparation is a determinant factor in the durability of an adhesive bond and to assess the effect of the applied pretreatments in the performance after aging, evaluation of the failure mode is the most important. Fig. 9b summarizes the results of the calculations obtained by Equation (1). As a general observation, there is a clear difference between the samples with the "only selected parameter", which shows a mixed failure without aging, and a full adhesive failure at the interface at all the salt spray exposure times. In contrast, the samples with sol-gel or sol-gel with primer, show a cohesive failure as the dominant failure mode with small areas of adhesive failure after the aging exposure. Fig. 9c summarizes the failure photographs corresponding to the different surface pretreatments during the evaluated aging times. For 0 weeks, (the non-exposed samples) the calculated percentages of remaining adhesive were 66%, 85%, and 86% for the samples S, SSG, and SSGP, respectively. For the sample with the selected parameter only, as discussed in section 3.4, a mixed failure mode is observed in the failure photograph. On the other hand, samples SSG and SSGP, show remarkably similar failure modes, with a cohesive failure. After 3 weeks of aging these values were reduced, and the failure photographs presented in Fig. 9c show, for the S sample, the result of the diffusion of moisture into the adhesive-adherend interface, resulting in adhesive failure (See Figs. S3 and S4). In contrast, the photographs of samples SSG and SSGP show only a slight reduction in the cohesive failure mode and reveal a very small area with adhesive failure, being a little smaller for the primed sample. The failure photographs of the S samples presented in Fig. 9c show that the moisture has penetrated the adhesive-adherend surface progressively until it reaches the centre, and at 12 weeks no adhesive can be seen visually on the adherend's surface. Finally, the samples treated with either sol-gel or sol-gel and primer, show the same cohesive failure characteristics within the standard deviation.

From the results above, the samples with the selected parameter only (S), allowed the largest moisture penetration on the interface. Park et al. [7] show that the diffusion of moisture into the adhesive–adherend interface result in hydration of the anodic oxide layer obtained by phosphoric acid containment systems (PACs). In this research, the oxide layer developed in the titanium alloy surface after UV/Ozone irradiation could have been hydrated, leading to adhesive plasticization and stress built up due to swelling, which finally displaces the adhesive from the substrate [37]. The moisture absorption also caused a big reduction in

the tensile strength. Roughly 20% of tensile strength was retained after 12 weeks of exposure time. On the contrary, both sol-gel and sol-gel with primer were shown as effective pretreatments to get a durable adhesive bond after 12 weeks of exposure time with mostly cohesive failure. The sol-gel observed performance was as expected due to the organosilane component that promotes superior bonding, and to the zirconium component that creates a strong covalent bond with the titanium and acts as an oxygen diffusion barrier that stabilizes the metal-resin interface providing an improved degree of corrosion resistance [17]. Adding the modified water–based epoxy primer to the sol-gel film ensures the coupling between the sol-gel and the adhesive enhancing the durability of the adhesive bond compared with the only sol-gel treated samples.

4. Conclusion

In this work, experiments were conducted to analyze the effect of both grit blasting and UV/Ozone surface pretreatments on Ti6Al4V substrates adhesively bonded and tensile strength tested. The effectiveness of *Si*–Zr sol-gel and a modified water-based epoxy primer on the durability of the adhesive bonds exposed to salt spray were studied. Based on these results, conclusions can be summarized as follows:

1. The Ti surface morphology can be influenced by different grit blasting pressures. An increase in pressure leads to an increase in surface roughness.
2. The metallic titanium surface was cleaned and oxidized by a UV/ozone treatment. XPS results showed that the higher the UV/Ozone irradiation time, the higher the Ti(IV) which, together with the removal of organic contamination, reduced the contact angle with water at both grit-blasting pressures studied.
3. The initial adhesive performance showed the same tensile strength in all the pretreatments studied. However, the fracture surface analysis showed that the roughest samples exposed to the highest UV/Ozone radiation time reached a higher percentage of remaining adhesive, showing the effectivity of UV/Ozone as a titanium surface pretreatment.
4. After salt spray exposure, the samples with the optimal selected parameter only, showed moisture penetration at the titanium interface, causing a strong reduction in the tensile strength after the highest salt spray exposure time and full adhesive failure. The samples with sol-gel and sol-gel combined with a primer showed a strongly improved aging behaviour with mostly cohesive failure.

Acknowledgements

This project is part of Work package 4 of the project 'Fieldlab Composieten Onderhoud & Reparatie: bouwen aan het DCMC' of the 1.B.1 innovation program OP Zuid 2014–2020 which is subsidized by the European Union and supported by the Provincie Noord-Brabant, of The Netherlands.

Furthermore, the authors would like to thank Cees Paalvast for applying primer and sol-gel, and all the staff of the Delft Aerospace Structures and Materials Laboratory and the DEMO University workshop for their collaboration during the realization of this project.

Appendix A. Supplementary data

Supplementary data to this article can be found online at https://doi.org/10.1016/j.ijadhadh.2020.102750.

References

[1] Baburaj EG, Starikov D, Evans J, Shafeev GA, Bensaoula A. Enhancement of adhesive joint strength by laser surface modification. Int J Adhesion Adhes 2007;27:268–76. https://doi.org/10.1016/j.ijadhadh.2006.05.004.
[2] Yu YS, Xie LS, Chen MH, Wang N, Wang H. Surface characteristics and adhesive strength to epoxy of three different types of titanium alloys anodized in NaTESi electrolyte. Surf Coating Technol 2015;280:122–8. https://doi.org/10.1016/j.surfcoat.2015.09.010.
[3] Mertens T, Gammel FJ, Kolb M, Rohr O, Kotte L, Tschöcke S, et al. Investigation of surface pre-treatments for the structural bonding of titanium. Int J Adhesion Adhes 2012;34:46–54. https://doi.org/10.1016/j.ijadhadh.2011.12.007.
[4] van Dam JPB, Abrahami ST, Yilmaz A, Gonzalez-Garcia Y, Terryn H, Mol JMC. Effect of surface roughness and chemistry on the adhesion and durability of a steel-epoxy adhesive interface. Int J Adhesion Adhes 2020;96:102450. https://doi.org/10.1016/j.ijadhadh.2019.102450.
[5] Li J, Li Y, Huang M, Xiang Y, Liao Y. Improvement of aluminum lithium alloy adhesion performance based on sandblasting techniques. Int J Adhesion Adhes 2018;84:307–16. https://doi.org/10.1016/j.ijadhadh.2018.04.007.
[6] Zain NM, Ahmad SH, Ali ES. Effect of surface treatments on the durability of green polyurethane adhesive bonded aluminium alloy. Int J Adhesion Adhes 2014;55:43–55. https://doi.org/10.1016/j.ijadhadh.2014.07.007.
[7] Park SY, Choi WJ. Investigation on the effectiveness of silane-based field level surface treatments of aluminum substrates for on-aircraft bonded repairs. Int J Adhesion Adhes 2019;95:102414. https://doi.org/10.1016/j.ijadhadh.2019.102414.
[8] Mehr ME, Aghamohammadi H, Abbandanak SNH, Aghamirzadeh GR, Eslami-Farsani R, Siadati SMH. Effects of applying a combination of surface treatments on the mechanical behavior of basalt fiber metal laminates. Int J Adhesion Adhes 2019;92:133–41. https://doi.org/10.1016/j.ijadhadh.2019.04.015.
[9] Brack N, Rider AN. The influence of mechanical and chemical treatments on the environmental resistance of epoxy adhesive bonds to titanium. Int J Adhesion Adhes 2014;48:20–7. https://doi.org/10.1016/j.ijadhadh.2013.09.012.
[10] Kurtovic A, Brandl E, Mertens T, Maier HJ. Laser induced surface nano-structuring of Ti-6Al-4V for adhesive bonding. Int J Adhesion Adhes 2013;45:112–7. https://doi.org/10.1016/j.ijadhadh.2013.05.004.
[11] Arnott D, Rider A, Mazza J. Chapter 3 - surface treatment and repair bonding. In: Baker AA, editor. Rose LRF, jones RBT-A in the BCR of MAS. Oxford: Elsevier Science Ltd; 2002. p. 41–86. https://doi.org/10.1016/B978-008042699-0/50005-X.
[12] Zhang Jin-sheng, Zhao Xu- hui, Zuo Yu, Xiong Jin- ping. The bonding strength and corrosion resistance of aluminum alloy by anodizing treatment in a phosphoric acid modified boric acid/sulfuric acid bath. Surf Coating Technol 2008;202:3149–56. https://doi.org/10.1016/j.surfcoat.2007.10.041.
[13] Correia S, Anes V, Reis L. Effect of surface treatment on adhesively bonded aluminium-aluminium joints regarding aeronautical structures. Eng Fail Anal 2018;84:34–45. https://doi.org/10.1016/j.engfailanal.2017.10.010.
[14] Molitor P, Barron V, Young T. Surface treatment of titanium for adhesive bonding to polymer composites: a review. Int J Adhesion Adhes 2001;21:129–36. https://doi.org/10.1016/S0143-7496(00)00044-0.
[15] He P, Chen K, Yu B, Yue CY, Yang J. Surface microstructures and epoxy bonded shear strength of Ti6Al4V alloy anodized at various temperatures. Compos Sci Technol 2013;82:15–22. https://doi.org/10.1016/j.compscitech.2013.04.007.
[16] Cobb TQ, Johnson WS, Lowther SE, St Clair TL. Optimization of surface treatment and adhesive selection for bond durability in Ti-15-3 laminates. J Adhes 1999;71:115–41. https://doi.org/10.1080/00218469908014844.

[17] Blohowiak Kay Y, Osborne Joseph H, Krienke KA. SOL FOR COATING METALS 1998. US patent 5,814,137.
[18] Callinan RJ, Galea SC. Advances in the bonded composite repair of metallic aircraft structure, 2; 2002. https://doi.org/10.1016/B978-008042699-0/50021-8.
[19] He P, Huang M, Fisher S, Yue CY, Yang J. Effects of primer and annealing treatments on the shear strength between anodized Ti6Al4V and epoxy. Int J Adhesion Adhes 2015;57:49–56. https://doi.org/10.1016/j.ijadhadh.2014.10.004.
[20] Kohli R. Applications of UV-ozone cleaning technique for removal of surface contaminants, 11. Elsevier Inc.; 2019. https://doi.org/10.1016/b978-0-12-815577-6.00009-8.
[21] Ramanathan S, Chi D, McIntyre PC, Wetteland CJ, Tesmer JR. Ultraviolet-ozone oxidation of metal films. J Electrochem Soc 2003;150:110–5. https://doi.org/10.1149/1.1566416.
[22] Ghoshal T, O'Connell J, Sinturel C, Andreazza P, Holmes JD, Morris MA. Solvent mediated inclusion of metal oxide into block copolymer nanopatterns: mechanism of oxide formation under UV-Ozone treatment. Polymer 2019;173:197–204. https://doi.org/10.1016/j.polymer.2019.04.043.
[23] Kim J, Wang J, Daineka D, Johnson EV. Improvement of near-infrared diffuse reflectance of silver back reflectors through Ag2O formation by a UV-ozone exposure process. Sol Energy Mater Sol Cells 2017;170:114–9. https://doi.org/10.1016/j.solmat.2017.05.067.
[24] Mathieson I, Bradley RH. Improved adhesion to polymers by UV/ozone surface oxidation. Int J Adhesion Adhes 1996;16:29–31. https://doi.org/10.1016/0143-7496(96)88482-X.
[25] Bok S, Lim GH, Lim B. UV/ozone treatment for adhesion improvement of copper/epoxy interface. J Ind Eng Chem 2017;46:199–202. https://doi.org/10.1016/j.jiec.2016.10.031.
[26] ASTM. Standard D2094-00 (2014): standard practice for preparation of bar and rod specimens for adhesion tests. ASTM Int; 2015. https://doi.org/10.1520/D2094-00R14.2.
[27] ASTM. Standard D7490-13: standard test method for measurement of the surface tension of solid coatings, substrates and pigments using contact angle measurements. ASTM Int; 2013. p. 1–5. https://doi.org/10.1520/D7490-13.2.
[28] ASTM. Standard D295-96 (2015): standard test method for tensile strength of adhesives by means of bar and rod specimens. ASTM Int; 2015. https://doi.org/10.1520/D2095-96R15.2.
[29] ASTM. Standard B117: standard practice for operating salt spray (fog). ASTM Int; 2011. https://doi.org/10.1520/B0117-11.2.
[30] Wenzel RN. Resistance of solid surfaces to wetting by water. Ind Eng Chem 1936;28:988–94. https://doi.org/10.1021/ie50320a024.
[31] Klonica M, Kuczmaszewski J. Modification of Ti6Al4V titanium alloy surface layer in the ozone atmosphere. Materials 2019;12. https://doi.org/10.3390/ma12132113.
[32] Hierro-Oliva M, Gallardo-Moreno AM, González-Martín ML. XPS analysis of Ti6Al4V oxidation under UHV conditions. Metall Mater Trans A Phys Metall Mater Sci 2014;45:6285–90. https://doi.org/10.1007/s11661-014-2570-0.
[33] Biesinger M, Payne B, Grosvenor A, Lau LW, Gerson A, Smart R. Resolving surface chemical states in XPS analysis of first row transition metals, oxides and hydroxides: Cr, Mn, Fe, Co and Ni. Appl Surf Sci 2011;257:2717–30. https://doi.org/10.1016/j.apsusc.2010.10.051.
[34] Lee TM, Chang E, Yang CY. Surface characteristics of Ti6Al4V alloy: effect of materials, passivation and autoclaving. J Mater Sci Mater Med 1998;9:439–48. https://doi.org/10.1023/A:1008815316564.
[35] Oliveira V, Sharma SP, de Moura MFSF, Moreira RDF, Vilar R. Surface treatment of CFRP composites using femtosecond laser radiation. Optic Laser Eng 2017;94:37–43. https://doi.org/10.1016/j.optlaseng.2017.02.011.
[36] He P, Chen K, Yang J. Surface modifications of Ti alloy with tunable hierarchical structures and chemistry for improved metal-polymer interface used in deepwater composite riser. Appl Surf Sci 2015;328:614–22. https://doi.org/10.1016/j.apsusc.2014.12.081.
[37] Pethrick RA. Design and ageing of adhesives for structural adhesive bonding-A review. Proc Inst Mech Eng Part L J Mater Des Appl 2015;229:349–79. https://doi.org/10.1177/1464420714522981.